13-7; I(R^1 = *m*-xylylene; R^2 = CH_3; R^3 = CH_3; B = py)·2PF_6, 87114-92-9; I(R^1 = *m*-xylylene; R^2 = CH_3; R^3 = CH_3, B = 1-Mim)·PF_6, 87114-93-0; I(R^1 = *m*-xylylene; R^2 = $CH_2C_6H_5$; R^3 = CH_3; B = py)·2PF_6, 87114-95-2; I(R^1 = *m*-xylylene; R^2 = CH_3; R^3 = *n*-C_7H_{15}, B = py)·2PF_6, 87114-97-4; I(R′ = *m*-xylylene; R^2 = CH_3; R^3 = C_6H_5; B = py)·2PF_6, 87114-99-6; I(R′ = *m*-xylylene; R^2 = CH_3; R^3 = C_6H_5, B = 1-Mim)·2PF_6, 87115-01-3; I(R^1 = *m*-xylylene; R^2 = $CH_2C_6H_5$; R^3 = C_6H_5, B = py)·2PF_6, 87115-03-5; I(R′ = *m*-xylylene; R^2 = $CH_2C_6H_5$, R^3 = C_6H_5; B = 1-Mim)·2PF_6, 87115-05-7; I(R′ = *m*-xylylene; R^2 = CH_3; R^3 = *p*-$MeOC_6H_4$; B = py)·2PF_6, 87136-01-4; I(R^1 = *m*-xylylene; R^2 = CH_3; R^3 = *p*-ClC_6H_4; B = py)·2PF_6, 87115-07-9; I(R^1 = *m*-xylylene; R^2 = CH_3; R^3 = *p*-FC_6H_4; B = py)·2PF_6, 87115-09-1; I(R^1 = $(CH_2)_5$;R^2 = CH_3; R^3 = C_6H_5; B = py)·2PF_6, 87115-11-5; H_2O, 7732-18-5; bis(acetonitrile)iron(II) chloride, 87114-91-8; bis(pyridine)iron(II) chloride, 15616-26-9.

Supplementary Material Available: Atomic coordinates and calculated and observed structure factors for both structures (29 pages). Ordering information is given on any current masthead page.

X-ray Absorption Spectra and the Coordination Number of Zn and Co Carbonic Anhydrase as a Function of pH and Inhibitor Binding

Vittal Yachandra,[†] Linda Powers,[‡] and Thomas G. Spiro*[†]

Contribution from the Department of Chemistry, Princeton University, Princeton, New Jersey 08544, and Bell Laboratories, Murray Hill, New Jersey 07974.
Received January 13, 1983

Abstract: X-ray absorption spectra are reported for native (Zn) and Co-reconstituted bovine carbonic anhydrase (CA), prepared at several pH values across the acid–alkaline transition and in the presence of inhibitors (acetazolamide, imidazole, acetate, HCO_3^-, NO_3^-, Cl^-, CN^-, OCN^-, SCN^-). The extended fine structure (EXAFS) was analyzed by filtering the first-shell contribution and was compared with a series of model compounds of known structure having various coordination numbers. Co-CA showed variable coordination, as revealed by the calculated number of scatterers and by the average bond distance: four-coordination for the alkaline form and for complexes with CN^- and acetazolamide, and five-coordination for the acid form and for complexes with acetate and bicarbonate. For Zn-CA, however, the average coordination number is independent of pH, or of inhibitor binding, and is judged to be four from the relatively short ~2.01-Å average first-shell distance, although the EXAFS-determined average coordination numbers were slightly higher and are less reliable than the distance as monitors of the Zn coordination. Two-atom fits to the filtered first-shell EXAFS data improved the agreement for Zn-CA, with pairs of distances suggesting a ~0.1-Å spread in the Zn–ligand bond lengths, but no improvement was obtained for Co-CA. All of the EXAFS Fourier transforms showed the outer-shell peaks attributable to imidazole ring atoms, at constant intervals from the first-shell peak, implying no alterations in the angle of the imidazole rings relative to the metal–imidazole bonds. The K-edge spectra showed prominent 1s → 3d absorption bands for four-coordinate Co-CA complexes, reflecting 4p–3d mixing in near-tetrahedral geometry; the band is attenuated in the five-coordinated species. The main Co edge peak is broader for the four-coordinate species. The Zn edge peak is distinctively split in Zn-CA, as it is in some four-coordinate Zn model compounds, possibly due to 4p, 4d, and/or 5p mixing. The energy of the second component decreases slightly as the pH is raised, following the pK_a for enzyme activation; the direction is that expected for ionization of a Zn-bound group, presumably H_2O. The Zn- and Co-CA coordination states are discussed in relation to the enzyme mechanism.

We have applied X-ray absorption spectroscopy to probe the coordination environment of the metal ion in zinc (native) and cobalt (reconstituted) carbonic anhydrase. This enzyme[1] is of fundamental biological importance, since it catalyzes the hydration–dehydration reaction of CO_2

$$CO_2 + H_2O \rightarrow HCO_3^- + H^+$$

Intensive structural and kinetic studies by many investigators[2] have shed much light on the enzyme, but key elements of the mechanism remain the subject of controversy.

X-ray crystallography[3] has established that the Zn^{2+} ion, which is essential for catalysis, is held by three histidine ligands and is coordinated by one, or possibly two, water molecules. The enzyme is active only in its alkaline form, and is inhibited by monovalent anions, which bind to the acid form.[1,4] The acid–alkaline transition has a pK_a of ~7, although exclusion of anions, including the commonly used SO_4^{2-}, appears to lower the intrinsic pK_a to ~5.[1,5] Zinc can be removed and replaced by other metal ions,[1] but only Co^{2+} gives significant CO_2 hydration activity, at a level ~50% of that of native enzyme. The visible absorption spectrum of the Co^{2+} enzyme changes markedly through the acid–alkaline transition and in response to inhibitor binding. The spectra are decidedly nonoctahedral in character, but they have otherwise been difficult to interpret in terms of coordination number and geometry. Only the tight-binding inhibitors CN^- and aromatic sulfonamides give tetrahedral-looking spectra, other forms of the enzyme giving spectra of less regular appearance. A weak band in the 1400-nm region has been interpreted by Bertini et al.[6] as arising from a five-coordinate structure. It is present in complexes with weakly binding inhibitors such as acetate, SCN^-, and NO_3^-, but appears to be lacking in the acid or alkaline form of the uncomplexed enzyme, suggesting four-coordination.[6] The acid–alkaline spectral change is mimicked by the Co^{2+} complex of [tris(3,5-dimethyl-1-pyrazolyl)methyl]amine, which has four N ligands and H_2O at a fifth position; the complex has a pK_a of ~9.[7]

[†] Princeton University.
[‡] Bell Laboratories.

(1) See Lindskog (Lindskog, S. In "Zinc Proteins"; Spiro, T. G., Ed.; Wiley: New York, 1982; Chapter 3 (in press)) for a current review.
(2) "Biophysics and Physiology of Carbon Dioxide"; Bauer, C., Gros, G., Bartels, H., Eds.; Springer Verlag: West Berlin, 1980.
(3) Kannan, K. K., in ref 2.
(4) Coleman, J. E., in ref 2.
(5) Koenig, S. H.; Brown, R. D.; Jacob, G. S., in ref 2, p 238.
(6) Bertini, I.; Canti, G.; Luchinat, C.; Scozzafava, A. *J. Am. Chem. Soc.* **1978**, *100*, 4873.

0002-7863/83/1505-6596$01.50/0

Likewise the Co^{2+} complex of [tris(4,5-dimethyl-2-imidazolyl)-methyl]phosphine oxide shows similar spectral changes upon anion binding or pH titration, with a pK_a of ~7.6.[8]

These model complexes, along with the observation that tetradentate macrocyclic complexes of Zn^{2+} can ionize a proton of coordinated H_2O with a pK_a as low as 8.1, have made chemically plausible the longstanding notion[10] that the activating pK_a of the enzyme is associated with the generation of Zn^{2+}-bound hydroxide. Lowering of the pK_a for coordinated water ionization is expected to result from a low coordination number and a hydrophobic environment, both of which are features of the active site. Various protein residues have also been advanced as candidates for this ionization, but they are all difficult to reconcile with the fact that inhibitor binding can shift the pK_a to very high values (>11),[1] an observation that is consistent with simple competitive binding between inhibitors and hydroxide. Most of the spectroscopic and kinetic evidence is consistent[1] with bound hydroxide being the nucleophile that attacks CO_2, although there has been some controversy about interpreting the relaxivity of the Co^{2+} enzyme for water protons.[1,6,11] The roles of the active-site residues and of the metal ion coordination group remain open questions.

It is to the last question that the current study is addressed. X-ray absorption spectroscopy, applicable to metalloproteins via synchrotron radiation, can provide valuable information about metal ion coordination environments through the energy and shape of the K shell absorption edges[12] and the frequency and amplitude of the post-edge extended fine structure (EXAFS).[13] The technique is applicable to both Co^{2+} and Zn^{2+}, providing a direct link between the two examples of metallo carbonic anhydrases. Because Zn^{2+}, with its $3d^{10}$ electronic configuration, is silent to most other forms of spectroscopy, it has generally been assumed that properties of the Co^{2+} enzyme apply as well as to the Zn^{2+} enzyme, although it has been recognized that differences may exist.[1] We find that the Zn^{2+} enzyme remains essentially four-coordinate in all its forms, although alterations in the K-edge shape imply differences in coordination geometry. The Co^{2+} enzyme, however, shows a definite propensity for five-coordination. This difference is of interest in connection with the likely involvement of a five-coordinate intermediate or transition state in the carbonic anhydrase mechanism.[14]

Experimental Section

Materials. Bovine carbonic anhydrase (Sigma or Miles Lab) was dialyzed against 50 mM Tris–sulfate or Bis-Tris–sulfate buffer, at various pH values, whose ionic strength was adjusted to 0.1 by addition of Na_2SO_4. The final protein concentration was 7–10 mM. Inhibitor complexes were prepared by adding the inhibitors to the dialysis solution at saturating concentrations. Cobalt carbonic anhydrase was prepared by adding stoichiometric amounts of $CoSO_4$ to the apoenzyme and dialyzing against buffer to remove any excess cobalt. The apoenzyme was prepared by dialyzing native enzyme against pyridine-2,6-dicarboxylic acid,[15] followed by extensive dialysis against buffer (pH 7.6) to remove excess chelating agent. The pH was measured, and enzyme activity was assayed,[16] before and after X-ray irradiation. No significant changes were observed.

The following reference compounds were prepared by literature methods: $[(ImH)_6Zn]Cl_2$[17] (ImH = imidazole), $(Py)_3Zn(NO_3)_2$[18] (Py = pyridine), $[(Py\text{-}O)_6Zn](ClO_4)_2$[19] (Py-O = pyridine *N*-oxide), $[(ImH)_4Zn](ClO_4)_2$,[20] $(ImH)_2Zn(Ac)_2$[21] (Ac^- = acetate), $Zn(His)_2\cdot 5H_2O$[22] (His = DL-histidine), $(ImH)_2ZnCl_2$,[23] $(Py)_2ZnCl_2$,[24] $[(Lut\text{-}O)_2]ZnCl_2$[25] (Lut-O = 2,6-lutidine *N*-oxide), $(ImH)_2CoCl_2$,[26] $(ImH)_2Co(Ac)_2$,[21] $[(Py\text{-}O)_6](ClO_4)_2$,[27] $[(Pic\text{-}O)_5Co](ClO_4)_2$[28] (Pic-O = 2-picoline *N*-oxide), and $[(ImH)_6Co](NO_3)_2$.[29]

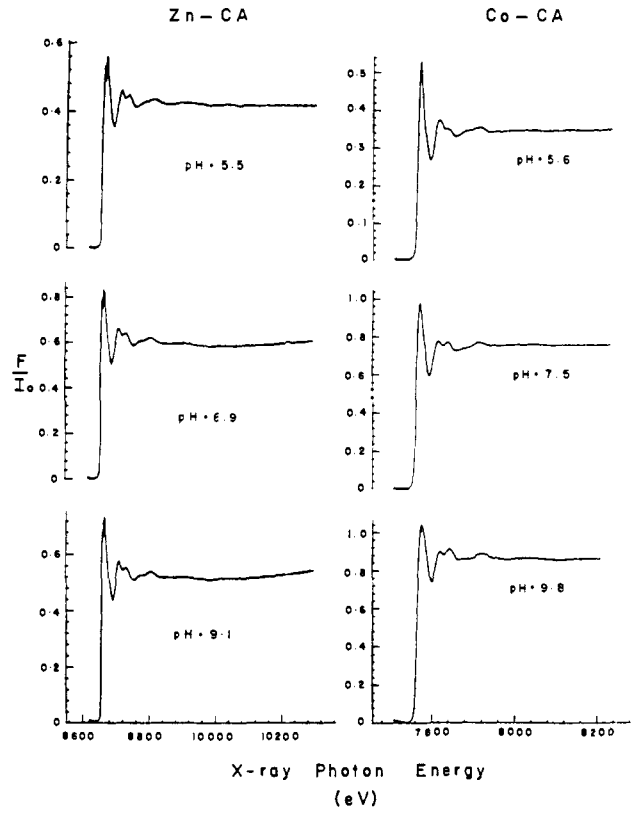

Figure 1. X-ray absorption spectra of zinc and cobalt bovine carbonic anhydrase (Zn-CA, Co-CA) as a function of pH. A linear background has been removed, which sets the absorption below the edge to zero. Data were collected by fluorescence, F, and I_0 is the incident intensity.

X-ray Measurements and Data Analysis. X-ray absorption spectra were obtained at the Stanford Synchrotron Radiation Laboratory (SSRL) during dedicated operation of the SPEAR storage ring, providing 40–80-mA electron beams at ~3.0 GeV. Co and Zn spectra were obtained with beam lines I-5 (unfocused, ~1×10^{10} photons/s with ~1-eV resolution), II-3 (focused, 6×10^{11} photons/s with ~3-eV resolution), and IV-2 (unfocused, 1×10^{12} photon/s with ~1-eV resolution), respectively. The signal was detected via the fluorescence emitted by the sample, with a filter–scintillation counter array.[30] The samples were mounted in Lucite holders, covered by Mylar film, and were inserted in a temperature-regulated N_2 cryostat, which permitted hemispherical X-ray exposure and fluorescence collection. Proteins were run as frozen solutions at ~100 °C, while the reference compounds were diluted with sucrose or $LiBF_4$ and run as solids, also at ~100 °C.

The data were analyzed with procedures used previously.[30,31,38] For

(7) Bertini, I.; Canti, G.; Luchinat, C.; Mani, F. *Inorg. Chim. Acta* **1980**, *46*, L91.
(8) Brown, R. S.; Salmon, D.; Curtis, N. J.; Kusuma, S. *J. Am. Chem. Soc.* **1982**, *104*, 3188.
(9) Wooley, P. *Nature (London)* **1975**, *258*, 677.
(10) (a) Davis, R. P. *J. Am. Chem. Soc.* **1959**, *81*, 5674. (b) Coleman, J. E. *J. Biol. Chem.* **1967**, *242*, 5212.
(11) (a) Jacob, G. S.; Brown, R. D.; Koenig, S. H. *Biochem. Biophys. Res. Commun.* **1978**, *82*, 203. (b) Bertini, I.; Canti, G.; Luchinat, C.; Messori, L. *Inorg. Chem.* **1982**, *21*, 3426.
(12) Shulman, R. G.; Yafet, Y.; Eisenberger, P.; Blumberg, W. E. *Proc. Natl. Acad. Sci. U.S.A.* **1976**, *73*, 1384.
(13) Eisenberger, P.; Kincaid, B. M. *Science (Washington, D.C.)* **1978**, *200*, 1441.
(14) (a) Pocker, Y.; Deits, T. L. *J. Am. Chem. Soc.* **1981**, *103*, 3949. (b) Pocker, Y.; Deits, T. L. *J. Am. Chem. Soc.* **1982**, *104*, 2424.
(15) Hunt, J. B.; Rhee, M-J.; Storm, C. B. *Anal. Biochem.* **1977**, *79*, 614.
(16) Armstrong, McD. J.; Meyers, D. V.; Verpoorte, J. A.; Edsall, J. T. *J. Biol. Chem.* **1966**, *241*, 5137.
(17) Sandmark, C.; Brändén, C. I. *Acta Chem. Scand.* **1967**, *21*, 993.
(18) Cameron, A. F.; Taylor, D. W.; Nuttall, R. H. *J. Chem. Soc., Dalton Trans.* **1972**, 1603.
(19) Carlin, R. J. *J. Am. Chem. Soc.* **1961**, *83*, 3773.
(20) Bear, C. A.; Duggan, K. A.; Freeman, H. C. *Acta Crystallogr., Sect. B* **1975**, *31B*, 2713.
(21) Horrocks, W. D., Jr.; Ishley, J.; Holmquist, B.; Thompson, J. S. *J. Inorg. Biochem.* **1980**, *12*, 131.
(22) Harding, M. M.; Cole, S. J. *Acta Crystallogr.* **1963**, *16*, 643.
(23) Edsall, J. T.; Felsenfeld, G.; Goodman, D. S.; Gurd, F. R. N. *J. Am. Chem. Soc.* **1954**, *76*, 3054.
(24) Steffen, W. L.; Palenik, G. J. *Acta. Crystallogr., Sect. B* **1976**, *32B*, 298.
(25) Sager, R. H.; Watson, W. H. *Inorg. Chem.* **1968**, *7*, 1358.
(26) Antti, C. J.; Lundberg, B. K. S. *Acta Chem. Scand.* **1972**, *26*, 3995.
(27) Bergendah, T. J.; Wood, J. S. *Inorg. Chem.* **1975**, *14*, 338.
(28) Byers, W.; Lever, A. B. P.; Parish, R. V. *Inorg. Chem.* **1968**, *78* 1835.
(29) Santoro, A.; Mighell, A. D.; Zocchi, M.; Reivmann, C. W. *Acta Crystallogr. Sect. B* **1969**, *25B*, 84.
(30) Powers, L.; Chance, B.; Ching, Y.; Angiolillo, P. *Biophys. J.* **1981**, *34*, 465.

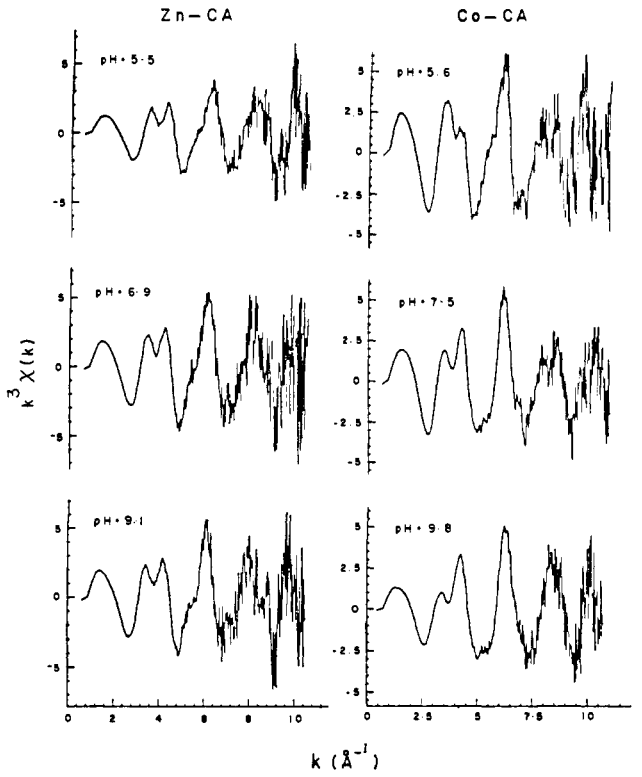

Figure 2. Background-removed Zn-CA and Co-CA EXAFS data, at various pH values, multiplied by k^3 and normalized by dividing by the edge height.

EXAFS analysis, many single scans were averaged after they were examined for satisfactory signal/noise, edge energy, and absence of anomalies. Monochromator settings were converted to energy, and a linear background was subtracted from these averaged data, which set the absorption below the edge to zero. Energy was then converted to wave vector, k, and the EXAFS was isolated by a cubic B-spline fit to remove the isolated atom or background contribution. Multiplication of these data by k^3 compensates for the approximate $1/k^3$ dependence of the EXAFS above $k \geq 4$ Å^{-1} and serves to somewhat equalize the oscillations over the observed k range. Fourier transformation of this background-subtracted, k^3-multiplied data produces a radial distribution of photoelectron backscattering[13] as a function of $R + \alpha(k)/2$, the distance from the absorbing atom plus the phase shift of the absorber–scatterer pair due to their respective potentials. The contribution that each shell makes to the EXAFS was isolated by Fourier filtering and back-transformation. The single shell contribution was then compared with a nonlinear least-squares fitting program to model compounds. This requires four parameters per atom type: average distance, R; number of scatterers, N; change of Debye–Waller contribution compared to the model compound, $\Delta\sigma^2$; and change of the edge or threshold compared to the model compound, ΔE_0 (=±2 eV). Significant correlation exists between N and $\Delta\sigma^2$ making the error in $N \sim 20\%$.[37] Values of R determined in this manner are ±0.02 Å.

Results

I. **EXAFS.** Figure 1 shows representative signal-averaged X-ray absorption spectra for Zn and Co carbonic anhydrase (CA), while Figure 2 shows the k^3-multiplied, background-subtracted EXAFS portion of the data. It can be seen in Figure 1 and more clearly in Figure 2 that the EXAFS modulation is essentially constant for the Zn-CA samples but varies significantly with pH for Co-CA.

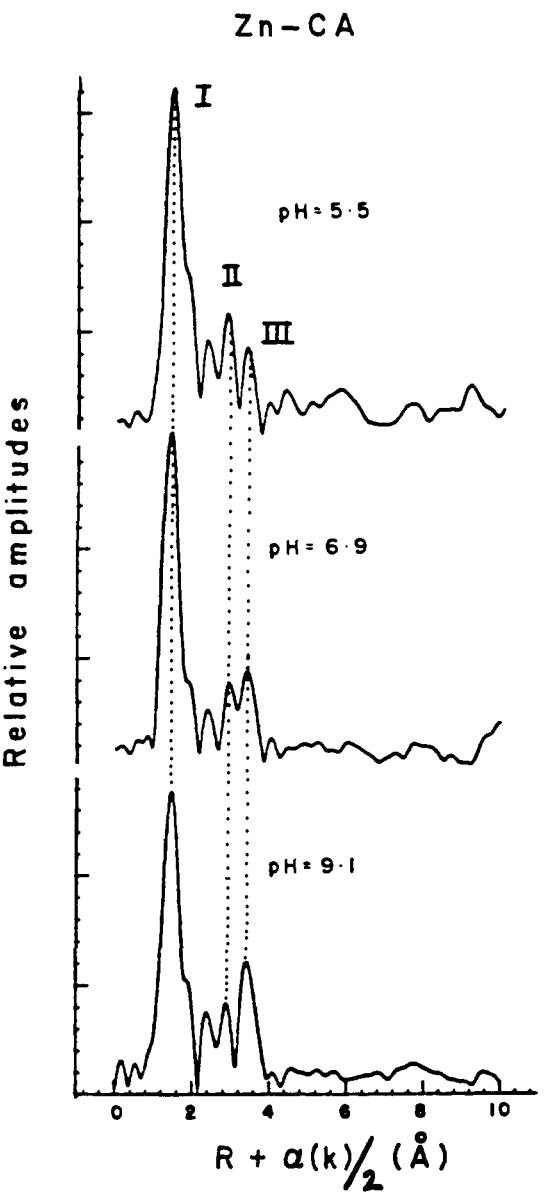

Figure 3. Fourier transforms of the $k^3 \times (k)$ data of the Zn-CA samples at different pHs.

Figures 3 and 4 show the Fourier transforms for the Zn and Co proteins at three pH values, spanning the activation pK_a (~7). The main peak, labeled I, is due to the scattering contribution of the nearest neighbor atoms (first shell) at a distance of ~2 Å. It can be seen at once that the position of this peak is constant for Zn-CA but shifts to higher $R + \alpha(k)/2$ (longer distance) for Co-CA, as the pH is lowered. The two outer peaks, labeled II and III, are attributable to the two sets of atoms, C2, C5 and N3, C5, of the imidazole ligands, which have well-defined distances beyond the first shell. They have been observed in EXAFS Fourier transforms of the Cu protein hemocyanin[31,32] and in Cu-imidazole compounds.[31,33] Their positions are constant for Zn-CA and shift to higher R at lower pH for Co-CA, in concert with the first-shell peak, with the distance between first shell and the second or third shell remaining constant.

Figure 5 shows the EXAFS modulation associated with only the first shell, obtained by filtering peak I from the Fourier transforms and back-transforming the filtered data. The constancy of the modulation phase for Zn-CA emphasizes the lack of distance change; small amplitude variations are seen, which are not, however, outside the likely experimental error. For Co-CA, the

(31) Brown, J. M.; Power, L.; Kincaid, B.; Larrabee, J. A.; Spiro, T. G. *J. Am. Chem. Soc.* **1980**, *102*, 4210.
(32) Co, M. S.; Hodgson, K. O.; Eccles, T. K.; Lontie, R. *J. Am. Chem. Soc.* **1981**, *103*, 984.
(33) Co, M. S.; Scott, R. A.; Hodgson, K. O. *J. Am. Chem. Soc.* **1981**, *103*, 986.
(34) Harding, M. H.; Cole, S. J., *Acta Crystallogr.* **1963**, *16*, 643.
(35) Citrin, P. H.; Eisenberger, P.; Kincaid, B. M. *Phys. Rev. Lett.* **1976**, *36*, 1346.
(36) Lee, P. A.; Citrin, P. H.; Eisenberger, P.; Kincaid, B. M., *Rev. Mod. Phys.* **1981**, *53*, 769.
(37) Eisenberger, P.; Lengler, B. *Phys. Rev. B* **1980**, *22*, 3551.
(38) Brown, J. M., Ph.D. Thesis, Princeton University, Princeton, NJ, 1978.
(39) Haffner, P. H.; Coleman, J. E. *J. Biol. Chem.* **1975**, *250*, 996.

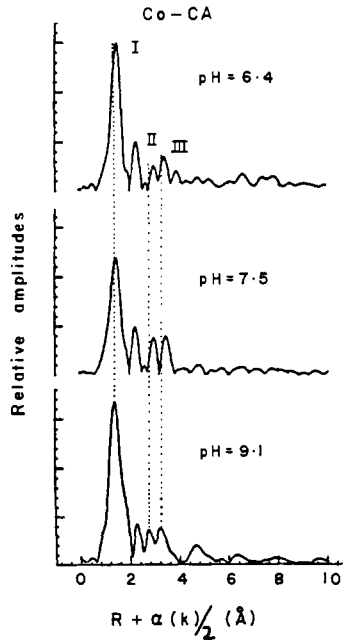

Figure 4. Fourier transforms of the $k^3 \times (k)$ data of the Co-CA samples at different pHs.

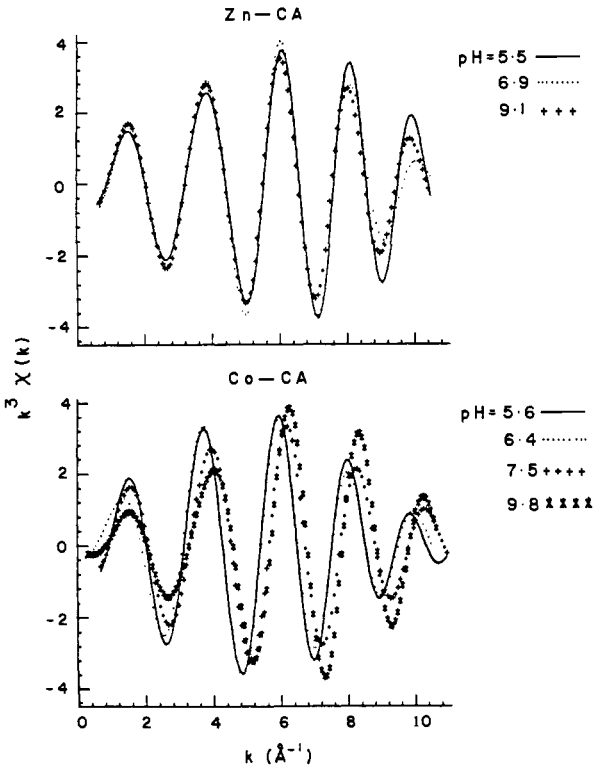

Figure 5. First-shell filtered data of Zn-CA and Co-CA as a function of pH.

increase in average distance with decreasing pH is again revealed by the evident change in the phase.

The filtered first-shell data were fit to the phases and amplitudes obtained from model compounds[13] allowing the average distance, R, number of scattering atoms, N, Debye–Waller factor, σ, and threshold energy, E_0, to vary.[31] For Zn-CA, the reference compound was $Zn(His)_2 \cdot 5H_2O$, with four nearly equal Zn–N bonds, of average distance 2.024 Å (range 2.000–2.047 Å);[34] for Co-CA, the reference compound was $[(Py\text{-}O)_6Co](ClO_4)_2$, with six 2.088-Å Co–O bonds.[27] The first-shell protein ligands are N and O, and the difference in phase and amplitude between N and O scatterers is too small to have any significant effect on the fitting parameters.[35,36]

Table I. Zn-CA Parameters from First-Shell Fourier-Filtered EXAFS Data[a]

pH of Zn-CA samples	R, Å[b]	N[c]	$\Delta\sigma^2 \times 10^{-3}$ [d]	ΔE_0, eV[e]
5.5	2.012	4.6	4.6	0.6
5.9	2.009	5.7	3.4	1.0
6.4	2.014	5.3	3.1	0.4
6.9	2.003	6.0	0.4	1.6
7.5	2.000	5.3	0.4	2.2
8.1	1.996	5.7	0.5	2.4
8.5	2.009	5.6	1.5	1.2
9.1	2.025	5.3	1.1	0.2
9.7	1.989	5.2	−1.5	2.2
lyophilized 8.5	2.035	5.4	−0.5	−0.4
Zn-CA + inhibitor[f]	**R, Å[b]**	**N[c]**	**$\Delta\sigma^2 \times 10^{-3}$ [d]**	**ΔE_0, eV[e]**
CN^-	2.010	5.7	−0.1	1.2
HCO_3^-	2.025	5.1	1.9	1.0
NO_3^-	2.021	5.6	3.2	1.2
Imh	2.022	5.3	2.1	0.4
Cl^- [g]	1.988 (N)	5.0	0.2	4.1
	2.292 (Cl)	2.9	5.6	−2.6

[a] The reference compound is $Zn(His)_2$. [b] R is the average distance ±0.02 Å. [c] N is the number of scattering atoms ±20%. [d] $\Delta\sigma^2$ is the change in the Debye-Waller factor, relative to the reference compound. [e] ΔE_0 is the change in edge energy relative to the reference compound. [f] The pH values of the inhibitor bound Zn-CA samples were as follows: CN^-, 7.5; HCO_3^-, 8.6; NO_3^-, 6.0; and Im, 8.5. [g] A two-shell fit using $Zn(His)_2$ for Zn–N and $ZnCl_2$ for Zn–Cl as reference compounds.

Table II. Co-CA Parameters from First-Shell Fourier-Filtered EXAFS Data[a]

pH of Co-CA samples	R, Å	N	$\Delta\sigma^2 \times 10^{-3}$	ΔE_0, eV
5.6	2.072	5.0	−5.0	0.4
6.4	2.058	5.3	−4.3	1.4
7.5	2.019	4.8	−3.2	−0.7
8.4	1.982	4.8	−1.1	2.2
9.8	2.004	4.3	0.4	−0.2
Co-CA + inhibitor[b]	**R, Å**	**N**	**$\Delta\sigma^2 \times 10^{-3}$**	**ΔE_0, eV**
CN^-	1.945	4.2	−2.0	−0.9
sulfonamide	1.983	3.6	2.4	0.9
HCO_3^-	2.094	3.6	−1.9	−3.6
NO_3^-	2.024	5.1	−5.5	1.0
Ac^-	2.111	5.2	−1.9	−2.1

[a] Symbols are as in Table I. The reference compound was $[(Py\text{-}O)_6Co](ClO_4)$. [b] The pH values of inhibitor bound Co-CA samples were as follows: CN^-, 7.6; sulfonamide, 8.7; HCO_3^-, 7.6; NO_3^-, 6.0; Ac^-, 6.0.

The results of the fitting procedure are given in Tables I and II. As expected from the curves, the average Zn-CA first-shell distance is invariant with pH, aside from small random fluctuations, with an average value of 2.01 Å. Likewise, the calculated number of scatters, N, shows fluctuations that are within the error of ~20% but no trend with pH; the average value is 5.4. Co-CA, on the other hand, gives an average distance of 2.01 Å at pH 7.5 and above, but the distance increases at pH 6.4 and 5.6 to 2.06 Å. Similarly, the calculated number of scatters, N, increases for Co-CA from ~4.5 at high pH to ~5.0 at low pH. Although this change is within the error of N and taken alone could not unambiguously be interpreted as a change in coordination number, the fact that it correlates systematically with the average distance change suggests a change in the coordination sphere at the activation pK_a.

Figures 6 and 7 show the filtered first-shell data for inhibitor complexes of Zn-CA and Co-CA. The fitting parameters are also listed in Tables I and II. We observe the same pattern of constant average distances (2.01–2.02 Å) and N values (~5.4) for Zn-CA, but variable distances (1.65–2.11 Å) and N values (4–5) for

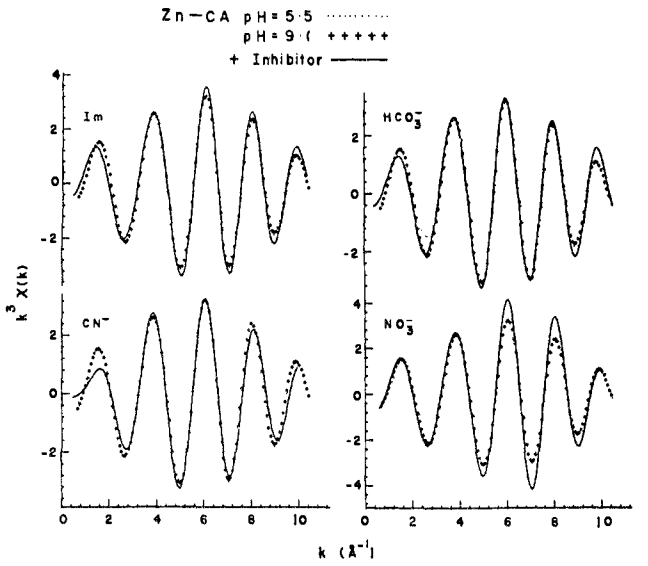

Figure 6. Comparison of the first-shell filtered data of Zn-CA at (···) pH 5.5 and (+ + +) pH 9.1 with that of the (—) inhibitor-bound enzyme. Im, imidazole-bound Zn-CA at pH 8.5; HCO_3^-, bicarbonate at pH 8.6; CN^-, cyanide at pH 7.5; NO_3^-, nitrate at pH 6.0.

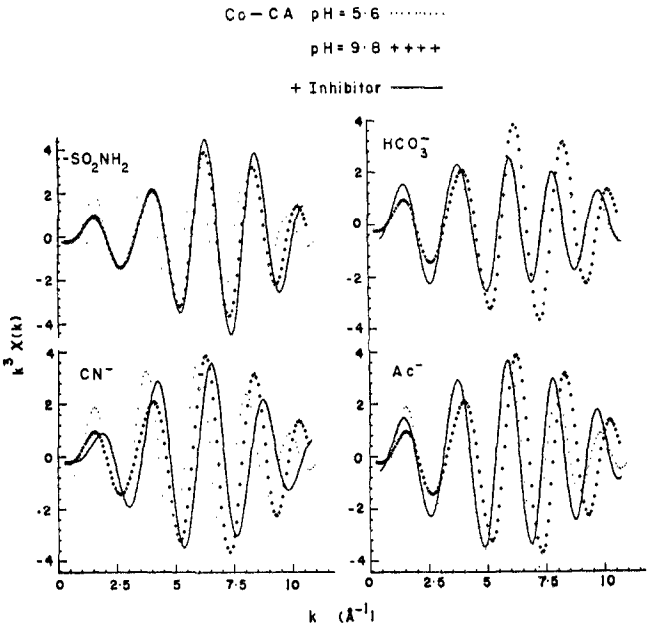

Figure 7. Comparison of the first-shell filtered data of Co-CA at (···) pH 5.6 and (+ + +) pH 9.8 with that of the (—) inhibitor-bound enzyme. $-SO_2NH2$, acetazolamide-bound Co-CA at pH 8.7; CN^-, cyanide at pH 7.6; HCO_3^-, bicarbonate at pH 7.6; Ac^-, acetate at pH 6.0.

Co-CA. Longer distances correlate with higher N values.

The calculated first-shell distances represent averages over the individual metal–ligand bond lengths. In order to explore the range of bond lengths consistent with the data, we carried out two-shell fits[38] to the filtered first-shell data, allowing for two classes of scatterers (N and O), each with its own distance, number, Debye–Waller factor, and E_0 shift. This procedure did not improve the fit for the Co-CA, and both best-fit distances were close to the previously determined single-shell distance. This was true even for the CN^- complex, which shows a rather short (1.945 Å) average first shell distance, that might have resulted from an appreciably shorter than average Co–CN distance. Apparently the strong field CN^- ligand contracts all of the Co ligand bonds slightly. For Zn-CA, however, the two-shell procedure reduced the sum of the squares of the residuals by an order of magnitude and gave two different distances, 1.93 and 2.03 Å. These values are not significant in and of themselves, since quite satisfactory fits can be obtained with a single average distance, or with other

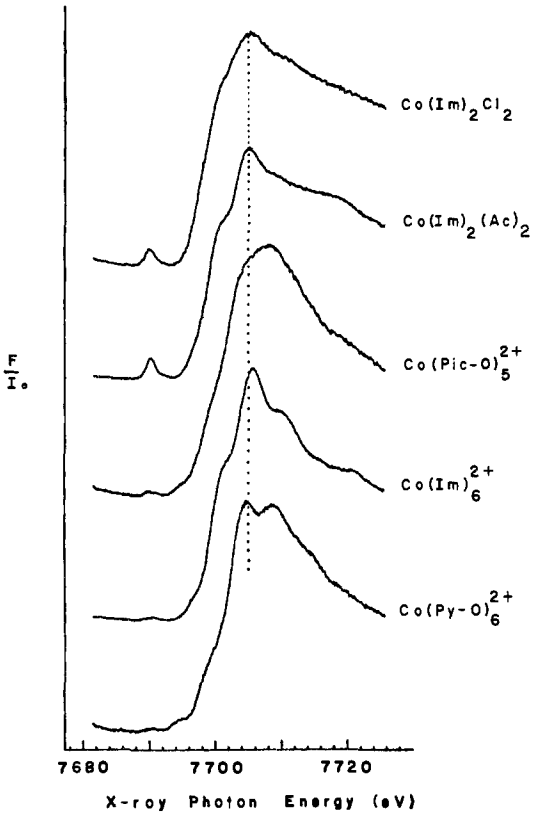

Figure 8. X-ray absorption K edges of Co in some 4-, 5-, and 6-coordinate complexes. Im = imidazole, Ac = acetate, Pic-O = 2-picoline N-oxide, Py-O = pyridine N-oxide.

pairs of distances between 1.93 and 2.03 Å. It does seem likely, however, that the Zn–ligand distances in Zn-CA vary over a range of ~0.1 Å, whereas the Co–ligand distances in Co-CA have a smaller spread.

A second distance within the first shell could be obtained reliably for the chloride complex of Zn-CA, Cl being a better scatterer, with a distinctly different phase, than N or O. The two-shell fit for this complex gave 1.99 Å for the N (or O) distance and 2.29 Å for the Cl distance. The latter value is in good agreement with standard Zn–Cl bond lengths, although the (Cl^-) Zn-CA crystal structure[3] has been reported to give a longer distance, 3.3 Å. A similar discrepancy was observed in the EXAFS study of (I^-)Zn-CA by Shulman and co-workers,[40] which gave a normal Zn–I distance of 2.65 Å, shorter than the crystallographically determined value of 3.7 Å.[3]

The imidazole outer shells, peaks II and III in the Fourier transforms, could in principle be analyzed to provide specific information about the imidazole ligands. The constancy in their positions, relative to the first-shell peak, implies no significant change in imidazole ring angles relative to the metal–imidazole bond. If the outer-shell amplitudes could be reliably related to the number of imidazole ligands, then the imidazole contribution to the first shell could be subtracted out by appropriate scaling, to allow more detailed analysis of the remaining ligands (water, hydroxide, or inhibitors). In studies of imidazole model compounds of Cu, Fe, Zn, and Co, however, the amplitudes of the outer-shell peaks show significant variations relative to one another and to the first-shell amplitude. This is seen strikingly in the Zn-CA Fourier transforms (Figure 3), in which the relative intensities of the outer-shell peaks become reversed as the pH changes. Since the peak positions do not differ, there is evidently no change in the radial geometry, and the intensity alterations must be due to multiple scattering effects, associated, perhaps, with changes in the imidazole orientations. The theory of multiple scattering[41]

(40) Brown, G. S.; Navon, G.; Shulman, R. G. *Proc. Natl. Acad. Sic. U.S.A.* **1977**, *74*, 1794.

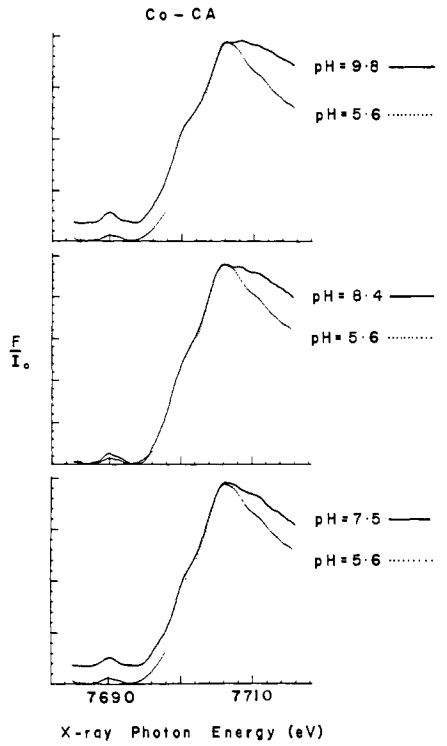

Figure 9. Comparison of Co K-edge spectrum of Co-CA at pH 5.6 (dotted line) with the spectra at pH 7.5, 8.4, and 9.8 (solid line).

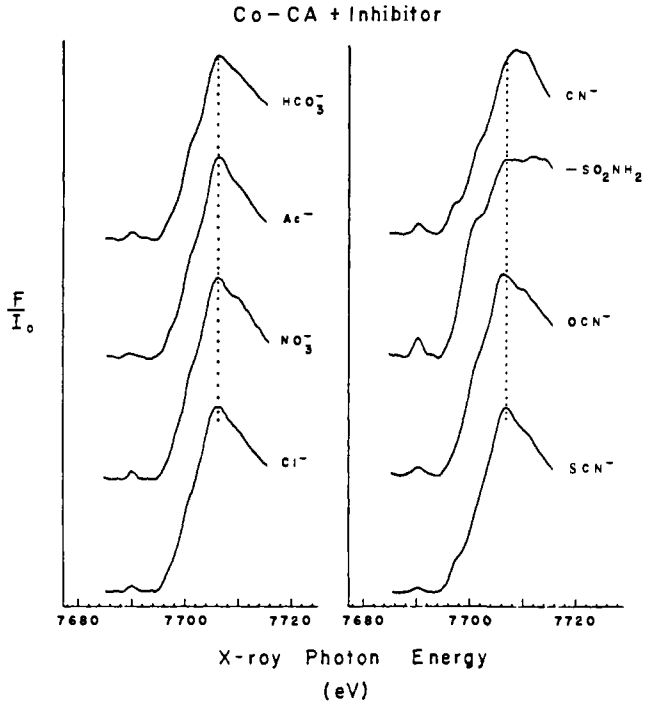

Figure 10. Co K-edge spectra Co-CA inhibitor complexes of HCO_3^- at pH 7.6, Ac^- at pH 6.0, NO_3^- at pH 6.0, Cl^- at pH 6.0, CN^- at pH 7.6, acetazolamide at pH 8.7, OCN^- at pH 7.3, and SCN^- at pH 6.0.

is insufficiently developed to allow the present situation to be analyzed with any confidence. We note that the imidazole group fitting procedure suggested by Hodgson and co-workers[33] would be inapplicable, since it implies constant relative amplitudes of the successive shells.

II. Edges. Figures 8–12 show X-ray absorption spectra in the region of the K edge for Co- and Zn-CA and their inhibitor complexes, as well as for several model compounds. It has long been recognized that for a given absorber the edge energy should correlate with the effective nuclear charge[42] and also that the structure of the spectrum may reflect excitation of the absorber to high-lying bound states.[12,42,44] It has generally been accepted that for first transition row metals the (forbidden) 1s → 3d transition can sometimes be seen as a small isolated peak below the edge, while the first major peak is assignable to the (allowed) 1s → 4p transition and a low energy shoulder may arise from the (forbidden) 1s → 4s transition.[12] Beyond the first major peak additional structure is often seen whose origin might lie in splittings of the 4p levels, mixing in of 4d character, and/or transitions to the 5p level.[43] The situation is not susceptible to a simple analysis, particularly as these high-lying orbitals overlap and interact with empty ligand orbitals. A recent theoretical study,[45] using SCF Xα calculations, suggested that all of the edge spectrum, beyond the 1s → 3d peak, is due to continuum levels, and that the structure is associated with "shape resonances".

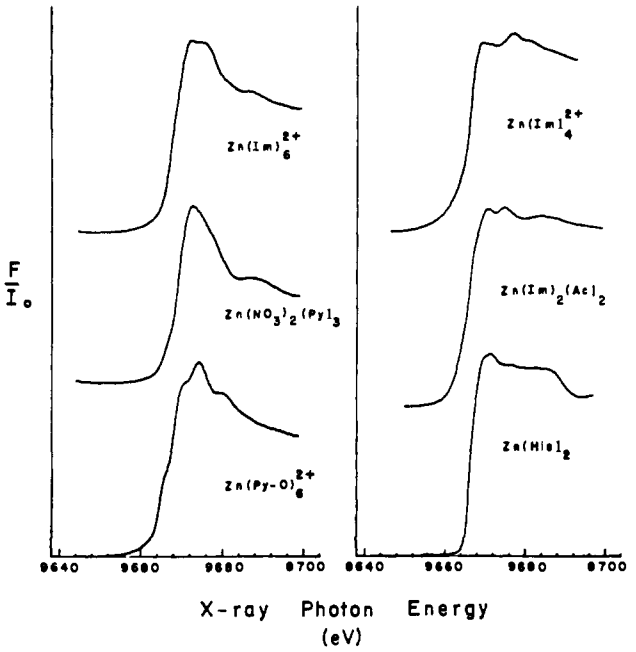

Figure 11. X-ray absorption K edges of Zn in some 4-, 6-, and 7-coordinate complexes, Py = pyridine, other symbols as in Figure 8.

Zn^{2+}, with a filled 3d subshell, cannot show a 1s → 3d peak, but this peak is seen in the Co^{2+} edge spectra. Its intensity is clearly related to the geometry of the complex, as shown in Figure 8. For the octahedral complexes $(ImH)_6Co^{2+}$ and $(Py\text{-}O)_6Co^{2+}$, the peak is barely observable, but it is pronounced in the tetrahedral complexes, $(ImH)_2CoCl_2$ and $(ImH)_2Co(Ac)_2$, which allow d–p mixing. The same intensification was observed by Shulman et al.[12] for the tetrahedral thiolate complex of Fe^{3+} in rubredoxin, relative to an octahedral reference compound. The five-coordinate, square-pyramidal complex $(PicO)_5Co^{2+}$ shows a 1s → 3d peak of intermediate intensity, implying some d–p mixing, although less than in a tetrahedral complex. The main edge peak also shows appreciable differences among this series of complexes, but the details are difficult to interpret. The overall trend is a broadening of the peak, with a flatter region at higher energies on going from six- to five- to four-coordination.

This trend is also seen in the Co-CA spectra (Figure 9). The 1s → 3d peak is seen at all pH's, but it grows and the main peak broadens as the pH is raised. Both changes are consistent with

(41) Teo, B. K. *J. Am. Chem. Soc.* **1981**, *103*, 3990.

(42) Ovsyannikova, I. A.; Batsonov, S. S.; Nasonova, L. I.; Batsonova, L. R.; Nekrasova, E. A. *Bull. Acad. Sci. USSR, Phys. Ser. (Engl. Transl.)* **1967**, *31*, 936.

(43) (a) Cotton, F. A.; Ballhausen, C. J. *J. Chem. Phys.* **1956**, *25*, 617. (b) Cotton, F. A.; Hanson, H. P. *J. Chem. Phys.* **1958**, *28*, 83.

(44) Srivastava, U. C.; Nigam, H. L. *Coord. Chem. Rev.* **1972**, *9*, 275.

(45) Kutzler, F. W.; Natoli, C. R.; Misemer, D. K.; Doniach, S.; Hodgson, K. O. *J. Chem. Phys.* **1980**, *73*, 3274.

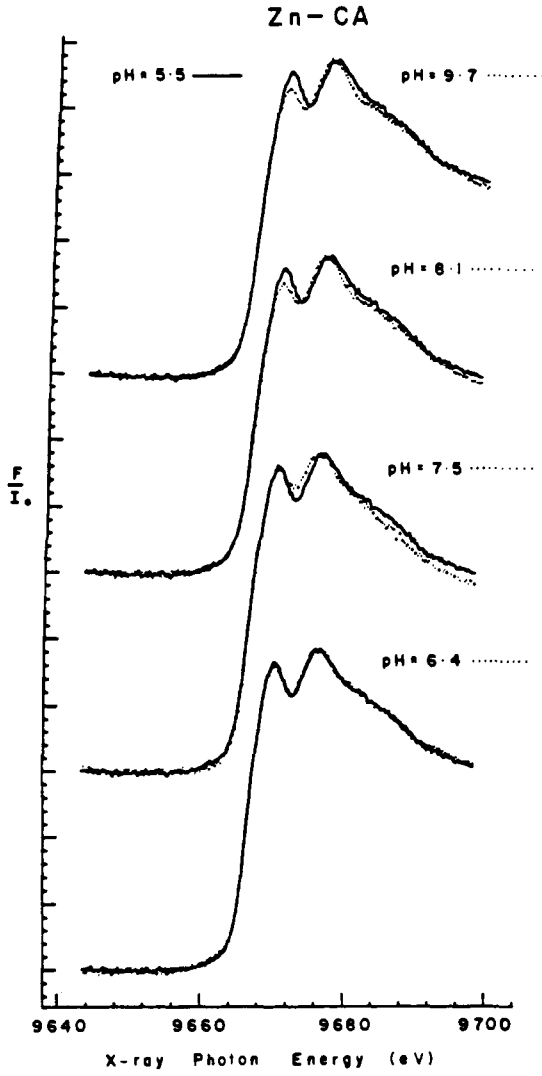

Figure 12. Zn-CA pH variation of the X-ray absorption K edge. The solid line is the edge spectrum at pH 5.5; it is overlayed on the edge spectra at pH 6.4, 7.5, 8.1, and 9.7, which are represented by dotted lines.

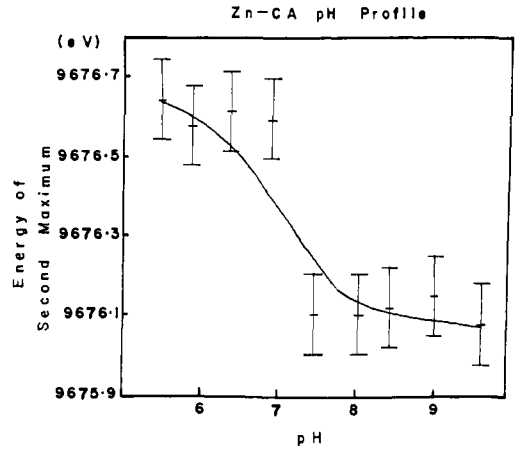

Figure 13. Zn K-edge second maximum energy (eV) vs. the pH of the Zn-CA.

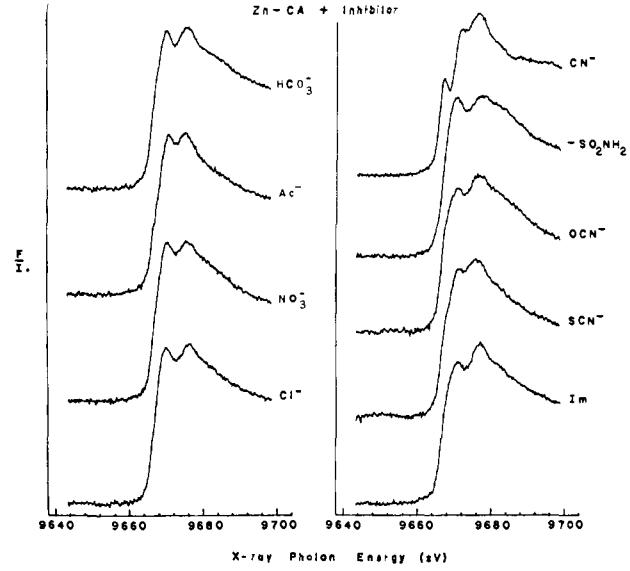

Figure 14. Zinc K-edge spectra of Zn-CA inhibitor complexes of HCO_3^- at pH 8.6, Ac^- at pH 5.9, NO_3^- at 6.0, Cl^- at pH 5.9, CN^- at pH 7.5, acetazolamide at pH 8.6, OCN^- at pH 7.3, SCN^- at pH 6.0, and imidazole at pH 8.5.

increasing tethedral character at high pH. Similar variations are seen for the Co-CA inhibitor complexes (Figure 10). The largest 1s → 3d peaks and the broadest main peaks are seen for the CN^- and sulfonamide complexes. The weakest 1s → 3d peaks are seen for the Ac^-, Cl^-, SCN^-, and HCO_3^- complexes, while the NO_3^- and OCN^- complexes are intermediate.

Because of the absence of the 1s → 3d peak, the Zn^{2+} edge spectra are less informative. Nevertheless reference compounds (Figure 11) again show broader peaks, flatter on the high energy side, for tetrahedral than for octahedral complexes, and a distinct splitting is sometimes seen, e.g., $(ImH)_4Zn^{2+}$. This splitting was also observed by Cotton and Hansen,[43b] who suggested that it might be due to 4p–4d mixing, and/or the involvement of the 5p level. The splitting is seen quite clearly in the edge spectra of Zn-CA (Figure 12). While the spectra are nearly invariant to pH, two slight but consistent trends can be observed; the first peak decreases in intensity while the second decreases in energy as the pH is raised. The second peak energy is plotted against pH in Figure 13 and is seen to follow satisfactorily the expected titration curve for enzyme activation. While such a small shift cannot reliably be interpreted, it is at least in the right direction if the Zn^{2+} charge is decreased by ionization of a ligand.

The Zn-CA inhibitor complexes (Figure 14) also show similar edge spectra. In the case of the sulfonamide inhibitor, however, a distinct broadening of the second peak is seen. For the CN^- complex, there is a pronounced low-energy shoulder, attributable to 1s → 4s, reminiscent of that seen[31] for the aqueous CN^- complex of (isoelectronic) Cu^+. It appears that CN^- is particularly effective at polarizing the filled 3d subshell, thereby inducing s–p mixing. Interestingly the ImH complex of Zn-CA shows a definite alteration in the intensity of the two edge peaks, although ImH is thought[46] to bind at a site 2.8 Å distant from the Zn^{2+}. Although no Zn–ImH bond appears to be formed, there is evidently a change in the Zn^{2+} coordination geometry sufficient to alter the edge structure.

Discussion

The EXAFS results indicate that the average coordination number of Co-CA decreases from low to high pH, as evidenced by the decrease in the calculated N value together with the decrease in the average first-shell distance (Table I). In Table III are assembled the bond distances available from crystal structures of Co^{2+} complexes with N and O ligands. A clear trend of increasing bond distance with increasing coordination number is seen. The range of EXAFS-determined distances for Co-CA (Table II), 1.98–2.07 (±0.02) Å, is bracketed by the reference compounds.

$(ImH)_2Co(Ac)_2$, although having only two Co–ImH bonds, is a good reference compound for alkaline Co-CA or for the sulfonamide complex. The Co–N (2.011 Å) and Co–O (1.975 Å) bonds average to 1.993 Å, the same value as determined for

(46) Kannan, K. K.; Petef, M.; Fridborg, K.; Cid-Dresdner, H.; Lövgren, S. *FEBS Lett.* **1977**, *73*, 115.

Table III. Zn and Co Models Crystallographic Data

	model	coordination	metal-ligand distances M-L	range, Å	av, Å	ref
		Zn				
7-coord	$(Py)_3Zn(NO_3)_2$	N_3O_4	Zn-N	2.129-2.201	2.165	18
			Zn-O	2.232-2.418	2.325	
6-coord	$[(Py\text{-}O)_6Zn](ClO_4)_2$	O_6	Zn-O		2.102	50
	$[(ImH)_6Zn]Cl_2$	N_6	Zn-N	2.153-2.264	2.203	17
4-coord	$Zn(DL\text{-}His)_2\cdot 5H_2O$	N_4	Zn-N	2.000-2.049	2.024	22
	$[(ImH)_4Zn](ClO_4)_2$	N_4	Zn-N	1.997-2.001	1.999	20
	$[(ImH)_2Zn]_\infty$	N_4	Zn-N		1.99	51
	$Zn(L\text{-}His)_2\cdot 2H_2O$	N_4	Zn-N		2.034	52
	$(ImH)_2ZnCl_2$	N_2Cl_2	Zn-N	1.995-2.020	2.008	53
			Zn-Cl	2.239-2.258	2.249	
	$[(ImH)_2Zn](Ac)_2$	N_2O_2	Zn-N		2.01	21
			Zn-O		1.96	
	$(Py)_2ZnCl_2$	N_2Cl_2	Zn-N	2.046-2.052	2.049	24
			Zn-Cl	2.215-2.228	2.222	
	$(Lut\text{-}O)_2ZnCl_2$	O_2Cl_2	Zn-O		2.01	25
			Zn-Cl		2.246	
	$(ImH)_2Zn(5,5\text{-}Et_2barb)_2$	N_4	Zn-N	2.009-2.023	2.016	54
		Co				
7-coord	$(Py)_3Co(NO_3)_2$	N_3O_4	Co-N	2.124-2.152	2.138	18
			Co-O	2.207-2.311	2.259	
6-coord	$[(Py\text{-}O)_6Co](ClO_4)_2$	O_6	Co-O		2.088	27
	$[(ImH)_6Co](NO_3)_2$	N_6	Co-N		2.160	55
	$[(ImH)_6Co](Ac)_2$	N_6	Co-N	2.151-2.188	2.168	56
	$[(ImH)_6Co]CO_3\cdot 5H_2O$	N_6	Co-N	2.161-2.182	2.172	57
	$(ImH)_2(H_2O)_2Co(CO_3)$	N_2O_4	Co-N		2.112	58
			Co-O	2.143-2.166	2.155	
	$Co(D\text{-}His)(L\text{-}His)\cdot 2H_2O$	N_4O_2	Co-N	2.077-2.141	2.118	59
			Co-O	2.067-2.152	2.110	
	$Co(L\text{-}His)_2\cdot H_2O$	N_4O_2	Co-N	2.11-2.19	2.17	60
			Co-O		2.12	
5-coord	$[(Pic\text{-}O)_5Co](ClO_4)_2$	O_5	$Co\text{-}O_{eq}$	1.97-1.99	2.03	61
			$Co\text{-}O_{ax}$	2.095-2.100		
4-coord	$(ImH)_2Co(Ac)_2$	N_2O_2	Co-N		2.011	21
			Co-O	1.974-1.977	1.976	
	$(ImH)_2CoCl_2$	N_2Cl_2	Co-N	1.987-1.989	1.988	26
			Co-Cl	2.237-2.264	2.251	
	$(ImH)_2Co(5,5\text{-}Et_2barb)_2$	N_4	Co-N	2.020-2.022	2.021	54

alkaline Co-CA (average of pH 8.4 and 9.8 determinations), and within experimental error of the value (1.983 Å) of the sulfonamide complex. (The distance for the CN^- complex, 1.945 Å, is slightly shorter, presumably due to polarization by the strong-field CN^- ligand; see Results section.) The best-fit N values are within experimental error of four, and the edge structures are tetrahedral in character. There is little doubt that alkaline Co-CA and the sulfonamide complex are in fact four-coordinate. One can conclude that, in addition to the three endogenous imidazole ligands, alkaline Co-CA has a single water or hydroxide ligand, which is replaced by a single ligand, presumably $-NH^-$, in the sulfonamide complex.

The crystal structure of the Zn-CA sulfonamide complex[47] is reported as showing five-coordinate Zn via coordination by sulfonamide O, as well as N atoms. But the second interaction (presumably O) must be too long (the distances are not reported) to contribute to the first-shell EXAFS data of either the Co-CA or the Zn-CA (vide infra) complex. Moreover the edge spectrum shows a prominent 1s → 3d peak for the Co-CA sulfonamide complex (Figure 10), as for $(ImH)_2Co(Ac)_2$ (Figure 8), implying tetrahedral coordination. Thus it seems unlikely that the interaction of the sulfonamide O atom with the Co^{2+} is electronically significant.

Acid Co-CA and the acetate and bicarbonate complexes have expanded coordination, as shown by increased N values and distances 2.06–2.11 Å (Table I). When allowance is made for averaging over Co–O and Co–N distances, these distances are lower than those expected for six-coordination (2.16–2.17 Å for Co–N in $(ImH)_6Co^{2+}$, 2.09 Å for Co–O in $(Py\text{-}O)_6Co^{2+}$; see Table III) and are consistent with five-coordination (2.03 Å for Co–O in $(Pic\text{-}O)_5Co^{2+}$). No five-coordinate Co–ImH distance is available, but it is expected to be 0.05–0.07 Å greater than Co–O, judging from the four- and six-coordinate complexes). The 1s → 3d band for these species is observable, but weak, as it is for trigonal-bipyramidal $(Pic\text{-}O)_5Co^{2+}$.

Thus there is evidently an equilibrium between five- and four-coordinate forms of Co-CA, high pH and sulfonamide binding favoring four-coordination, low pH and acetate or bicarbonate binding favoring five-coordination. These observations are in accord with Bertini et al.'s interpretation[6] of the optical absorption spectra, the observation of the ~1400-nm band assigned to five-coordinate species correlating well with the EXAFS and K-edge indicators. Previously the acid → alkaline optical changes had been suggested to reflect a four- → five-coordinate transition,[6] but the present results support Bertini et al.'s analysis; it is the alkaline form which is four-coordinate.

The optical absorption of the alkaline form, however, shows much greater splitting than expected of a regular tetrahedral complex;[6] the spectrum of the sulfonamide complex is more tetrahedral in appearance. Moreover the 1s → 3d peak is less intense for alkaline Co-CA (Figure 9) than for the sulfonamide complex (Figure 10) or for $(ImH)_2Co(Ac)_2$ (Figure 8), indicating a distortion from tetrahedral geometry for the four-coordinate alkaline Co-CA.

Bertini et al.[6] reported evidence for an equilibrium mixture of four- and five-coordinate forms of the chloride complex of Co-CA, the intensity of the ~1400-nm band varying with temperature. The present results suggest a similar mixture for the NO_3^- complex, which shows an intermediate first-shell distance (Table I)

(47) Kannan, K. K.; Vaara, I.; Notstrand, B.; Lövgren, S.; Borelll, A.; Fridborg, K.; Petef, M. "Proceedings on Drug Action at the Molecular Level"; Roberts, C. G. K., Ed.; MacMillan: New York, 1977, p 73.

(48) Nyman, P. O.; Lindskog, S. *Biochim. Biophys. Acta* **1964**, *85*, 141.

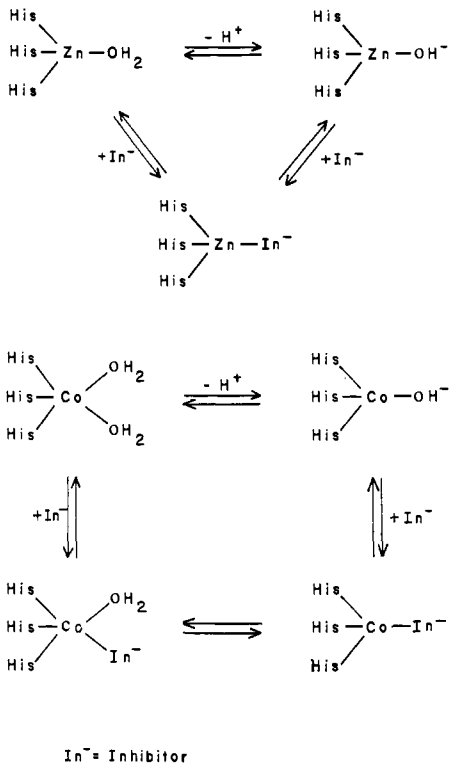

Figure 15. Scheme of the coordination changes in Zn-CA and Co-CA on changing pH and on binding to inhibitors (In^-).

and an intermediate 1s → 3d intensity (Figure 10). Considering its structural similarity to acetate and bicarbonate, it is surprising that nitrate should show a greater tendency toward four-coordination. Possibly the greater H-bonding propensities of $CH_3CO_2^-$ and HCO_3^-, both of which are stronger bases than NO_3^-, provide for stabilization of the five-coordinate structure.

These trends are not seen for Zn-CA, which gives an average first-shell distance within 0.01 Å of 2.01 Å, regardless of pH or inhibitor binding (except for heavy atom inhibitor ligands, such as Cl^-). Thus Zn^{2+} in CA does not appear to share the coordination flexibility of Co^{2+}, although four-, six-, and seven-coordinate Zn^{2+} complexes are known (see Table III). The 2.01-Å average distance is in the range of four-coordinate Zn–N and Zn–O distances (2.05–1.96 Å, Table III) and far below the six-coordinate distances (2.10–2.26 Å). (Unfortunately no crystal structures appear to have been determined for five-coordinate Zn^{2+} complexes.) Consequently it appears that Zn^{2+} remains four-coordinate in all forms of Zn-CA. The Zn-CA edge spectrum does show some variability, especially upon inhibitor binding, consistent with slight alterations in the ligand field, and possibly in geometry.

The X-ray absorption results shed little light on the nature of the ionization associated with the acid–alkaline transition of either Zn-CA or Co-CA. The slight energy lowering of the second edge peak of Zn-CA is in the right direction for ionization of a ligand bound to Zn^{2+}, but there is no basis for assessing the extent of the expected shift. We had thought that ionization of bound H_2O would produce a shortening of the Zn–O or Co–O bond, but the available crystal structures fail to establish a significant difference between metal–H_2O and metal–OH^- distances (e.g., tetrahedral Zn–OH and Zn–OH_2 distances of 1.95 Å are reported for $Zn_5(OH)_8(NO_3)_2 \cdot 2H_2O$[49]).

The results on coordination numbers and geometry, which are summarized in Figure 15, are relevant to the mechanism of CA catalysis. Since Zn-CA appears to be four-coordinate, product release requires an associative mechanism, with incoming solvent producing a five-coordinate intermediate or transition state prior to displacement of HCO_3^-, assuming, as seems likely, that CO_2 hydration does produce Zn-bound HCO_3^-. That a five-coordinate species is catalytically important has recently been suggested by Pocker and Deits,[14a,b] who found that anions inhibit Zn-CA uncompetitively at high pH, implying that in the presence of CO_2, the anions bind without displacement of the attacking OH^- group. Since the resulting complex is inhibitory it was suggested that HCO_3^- release requires proton transfer via an incoming water molecule at the fifth coordination site.

It remains important for a mechanism of this sort that the ground state of the enzyme be four-coordinate. The fact that Co-CA, unlike Zn-CA, becomes five-coordinate when HCO_3^- is bound may be related to the ~2-fold reductions in CO_2 hydration activity for Co-CA relative to Zn-CA.[48] The stability of the expanded coordination group may lower the driving force and slow the rate for product release. This factor is more important for other divalent ions (none of which show CO_2 hydration activity when substituted in CA), for which four-coordination is energetically less feasible than for Zn^{2+} or Co^{2+}.

Acknowledgment. This work was supported in part by NIH Grant GM 13498. Synchrotron radiation time was provided by the Stanford Synchrotron Radiation Laboratory, supported by NSF Grant DMR 77-27489, in cooperation with the Stanford Linear Accelerator Center and the U.S. Department of Energy.

(49) Stahlin, W.; Oswald, H. R., *Acta Crystallogr., Sect. B* **1970**, *26B*, 860.
(50) O'Connor, C. J.; Sinn, E.; Carlin, R. L. *Inorg. Chem.* **1977**, *16*, 3314.
(51) Stranberg, B.; Svensson, B.; Bränden, C. I., personal communication quoted in: Freeman, H. C. *Av. Protein Chem.* **1967**, *22*, 257.
(52) Kistenmacher, T. J. *Acta Crystallogr., Sect. B* **1972**, *B28*, 1302.
(53) Lundberg, B. K. S., *Acta Crystallogr.* **1966**, *21*, 901.
(54) Wang, B. C.; Craven, B. M. *Chem. Commun.* **1971**, 290.
(55) Prince, S.; Mighell, A. D.; Reiman, C. W.; Santoro, A. *Cryst. Struct. Commun.* **1972**, *1*, 247.
(56) Gadet, P. A.; Soubeyran, O. L. *Acta Crystallogr., Sect. B* **1974**, *B30*, 716.
(57) Strandberg, R.; Lundberg, B. K. S. *Acta Chem. Scand.* **1971**, *25*, 1767.
(58) Baraniak, E.; Freeman, H. C.; James, J. M.; Nockolds, C. E. *J. Chem. Soc. A* **1970**, 2558.
(59) Cardlin, R.; Harding, M. M. *J. Chem. Soc. A* **1970**, 384.
(60) Harding, M. M.; Long, H. A. *J. Chem. Soc. A* **1968**, 2554.
(61) Coyle, B. A.; Ibers, J. A. *Inorg. Chem.* **1970**, *9*, 767.